JOURNAL OF MATERIALS SCIENCE 27 (1992) 2383–2388

Electrical resistivity in the titanium carbonitride–zirconia system

E. BARBIER, F. THEVENOT
Laboratoire Céramiques Spéciales, Ecole Nationale Supérieure des Mines de Saint-Etienne, 158, cours Fauriel 42023 Saint-Etienne Cédex 2, France

A mixture of conductive titanium carbonitride and insulating partially stabilized zirconia powders was hot-press sintered, and a theoretical dense composite material obtained. The electrical conductivity as a function of C/N ratio and up to 50 vol % dispersed zirconia, partially stabilized by 3–5 mol % yttria, was studied. The Landauer model was tested. For low sintering temperatures (1500 °C), and with 3 mol % yttria in zirconia, titanium carbonitride particles present bad electrical contacts, and the transformation of tetragonal to monoclinic zirconia induces microcracking, therefore the Landauer model is not followed. On the other hand, for high-temperature (1700 °C) sintering, and using a fully stabilized zirconia powder with 5 mol % yttria, good electrical contacts between grains are established, thus the Landauer's model is confirmed. The high electrical conductivity of this insulator-conductive ceramic–ceramic composite allows an electric discharge machining.

1. Introduction

The solid solution $TiC_{1-x}N_x$ has attractive properties such as a high melting point, good hardness, and good thermal and electrical conductivity [1]. Titanium carbonitride is used for cutting tools [2] and wear-resistant materials, but the brittleness and high sintering temperature of TiCN as a pure phase pose problems for its use under high stress fields. So TiCN is mixed with other elements which could be metals (Mo, Ni Co) [3] or ceramics (TiB_2, Cr_3C_2) [2, 4]. In previous studies [5, 6] it has been found that adding ZrO_2 can improve the bending strength, fracture toughness and sinterability of TiCN.

This paper is devoted to the study of the electrical resistivity of the hot-pressed $TiC_{1-x}N_x$–ZrO_2 composites ($0 < x < 1$) containing less than 50 vol % of TZP (3 mol % Y_2O_3). The high electrical conductivity of these composites permits us to machine them easily using electrical discharge machining, which is a convenient and cheap way for preparing complex ceramic pieces. A theoretical model is sought for the description of composite resistivity, and the phenomena causing a discrepancy between experimental and theoretical values of electrical resistivities are explained.

2. Experimental procedure

The starting powders are supplied by H. C. Starck (Germany) for TiC, TiN, $TiC_{0.33}N_{0.67}$, $TiC_{0.5}N_{0.5}$ and $TiC_{0.67}N_{0.33}$ with mean particle sizes of 1.35, 1.6, 1.2, 1.7 and 1.6 μm, respectively. The two zirconia powders employed in the study called 3Y12 and 3Y6 (Pechiney, Criceram), had surface areas of 12.7 and 8.5 $m^2 g^{-1}$ and mean agglomerate sizes of 0.48 and 0.7 μm, respectively. Both contained 3 mol % yttria.

2.1. Preparation of powders

To describe electrical resistivity using a theoretical model, the material must behave as a quasi-homogeneous solid with its own properties on a macroscopic scale. So it is necessary to obtain a uniform dispersion of ZrO_2 particles by a good mix of the starting powders. Powder batches of 100 g were prepared according to the process shown in Fig. 1. To help the

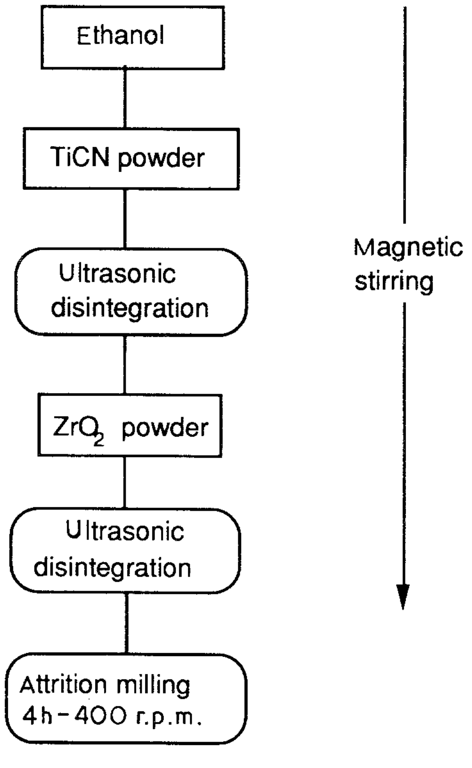

Figure 1 Elaboration process algorithm.

0022-2461 © 1992 Chapman & Hall

disagglomeration, we used an ultrasonic disintegration stage. Attrition milling was carried out in a 500-ml vessel coated with an organic material. 1100 g of zirconia milling balls (fully stabilized by MgO) of about 2 mm diameter and a Teflon coated rotor with a 400 r.p.m. velocity were used. A milling time of 4 h was chosen in accordance with a good dispersion and grain-size fineness. X-ray fluorescence showed an addition of ZrO_2 picked up from the milling balls. After attrition the mixture was vacuum dried and sieved.

2.2. Hot-pressing technique

Powder samples (16–18 g) were first cold-compacted in a graphite die (20 mm inner diameter) and uniaxially hot pressed in a (VS Pgr 7/10) laboratory press Degussa using a graphite resistor. The press was fully controlled and monitored by computer (temperature, pressure, shrinkage).

A first hot-pressing was performed for all the mixtures under 40 MPa in N_2 atmosphere to determine the maximum densification rate and the end of sintering. These data allowed us to execute a second hot-pressing cycle. A typical cycle consisted of heating and cooling rates of 30 °C min^{-1}; a soaking temperature fixed between the temperature of the maximum densification rate and the temperature at the end of sintering; a soaking time of 15 min; a 40-MPa pressure applied for 1000 °C to the end of the soaking time; and a nitrogen atmosphere. With these hot-pressing cycles, samples with more than 98% theoretical density were elaborated.

2.3. Sample characterization

Once hot-pressed, the sample densities were evaluated and the XRD pattern showed the monoclinic zirconia content after sintering. Then samples were cut into four bars of $3 \times 4 \times 17\ mm^3$, and the electrical resistivity measured by the four linear points method on the four bevelled edges of each bar, with a good reproducibility and stability.

3. Electrical conductivity models

The purpose of this study is to predict the conductivity of a $TiC_{1-x}N_x$–ZrO_2 composite according to nitrogen content x and to the volumic fraction of the phases. In the considered domain (Fig. 2), the validity of the model used to describe the conductivity is verified by comparing theoretical and experimental values for test compositions regularly distributed in the whole domain. In reality, the test compositions are different because of the additional ZrO_2 pick-up from milling balls.

The difference between the conductivity of the two considered phases (TiCN and ZrO_2) is so large that we are unlikely to achieve a good approximation using the conventional Wiener's [7] or Hashin–Shtrickman's [8] bounds, unless the microstructure of the composite is the same as that described by these bounds. Fig. 3 shows these bounds for a ratio between the conductivity σ_1 and σ_2 of the phases of 10^{10}.

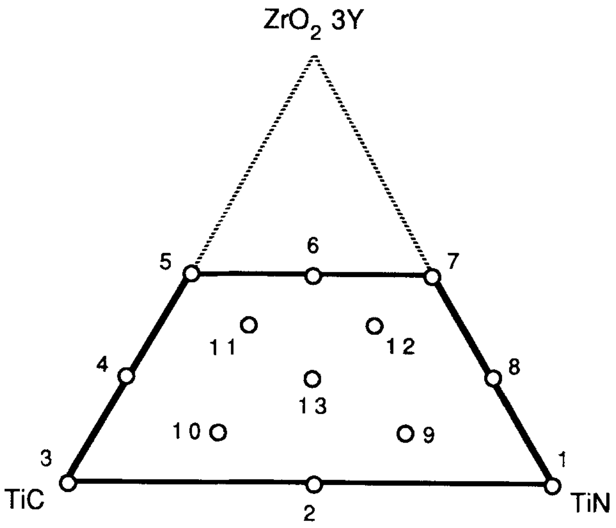

Figure 2 Domain studied into the $TiC_{1-x}N_x$–ZrO_2 system, and positions of the thirteen compositions elaborated.

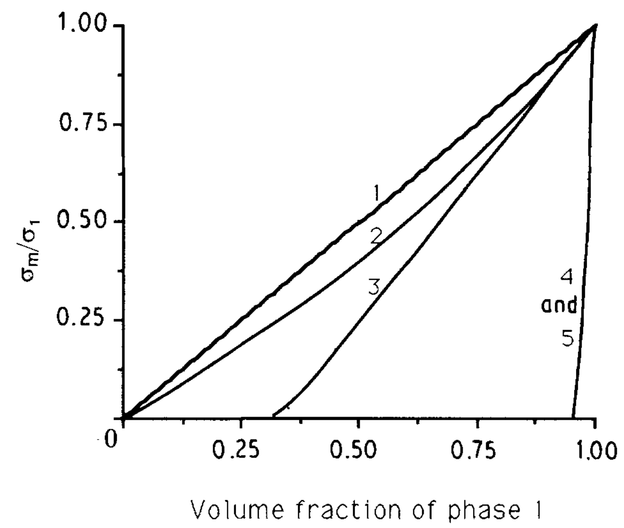

Figure 3 Conductivity evolution of a binary mixture with the volumic fraction of phase 1 when $\sigma_1/\sigma_2 = 10^{10}$. Curves 1 and 5 are Wiener's bounds, 2 and 4 Hashin–Shtrickman's bounds, and the curve 3 Landauer's model.

Wiener's bounds describe a material made from alternating laminae of both phases. A microstructure of a $TiC_{0.33}N_{0.67}$–18.5% ZrO_2 (Fig. 4) shows that the geometry of the studied composites is a random dispersion of which we will consider as spheres of the two phases. The Hashin–Shtrickman bounds describe a material where a spherical particle of one phase is completely embedded in a shell of the second phase, which is considered as surrounded by a homogeneous medium whose conductivity is composite (Fig. 5). The material studied does not follow this description, because its microstructure shows that even for low ZrO_2 content a grain of one type is often surrounded by grain of both types.

To build his model, Landauer [9] considered that a particle of one phase is surrounded by particles of both phases, which are imagined to be replaced by a uniform medium whose conductivity is that of the composite. This describes correctly the elaborated composite. So the Landauer's model is chosen to

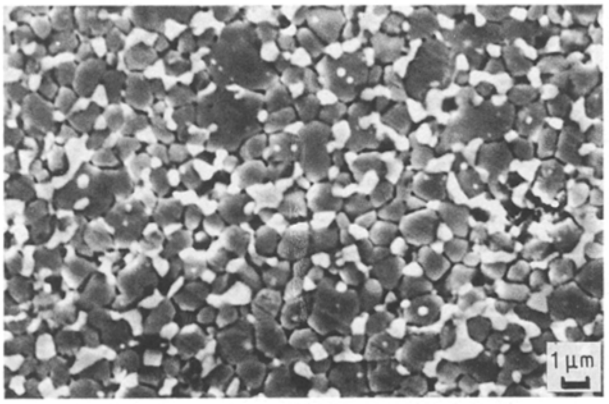

Figure 4 Microstructure (×4500) of the $TiC_{0.33}N_{0.67}$–18.5 vol % ZrO_2 composition.

predict the conductivity (nor resistivity) of the TiCN–ZrO_2 composites.

The conductivity of the composite σ_m is expressed as

$$\sigma_m = \frac{1}{4}[A + (A^2 + 8\sigma_1\sigma_2)^{1/2}] \qquad (1)$$

with $A = (3V_1 - 1)\sigma_1 + (3V_2 - 1)\sigma_2$, where σ_1, σ_2, V_1 and V_2 are the conductivity and the volumic fraction of phases 1 and 2, respectively.

If phase 1 is a conductor and phase 2 an insulator, the previous equation can be simplified and becomes

$$\sigma_m = \sigma_1\left(\frac{3V_1 - 1}{2}\right) \qquad (2)$$

The main drawback of the Landauer model is a false prediction of the volume content of the conductor for the percolation threshold of the conductivity: for $V_1 = 1/3$, $\sigma_m = 0$. However this is not important in this study, as the volumic fraction of conductor used in the composites is higher than the volumic fraction of conductor generally observed for the percolation threshold.

4. Results and discussion

Firstly, we measured the $TiC_{1-x}N_x$ phase conductivity against x. This property follows approximately Vegard's law (Fig. 6). Hence the $TiC_{1-x}N_x$ conductivity can be written as dependent on TiC conductivity ($\sigma_{TiC} \approx 14000\,\Omega^{-1}\,cm^{-1}$), TiN conductivity ($\sigma_{TiN} \approx 24000\,\Omega^{-1}\,cm^{-1}$) and x

$$\sigma_{TiC_{1-x}N_x} = (1 - x)\sigma_{TiC} + x\sigma_{TiN} \qquad (3)$$

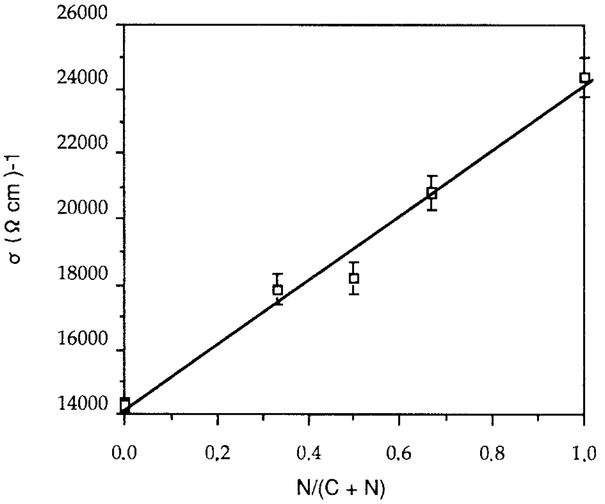

Figure 6 Variation of the conductivity with the nitrogen ratio of $TiC_{1-x}N_x$. $\sigma = 14130 + 10000x$; $R = 0.99$.

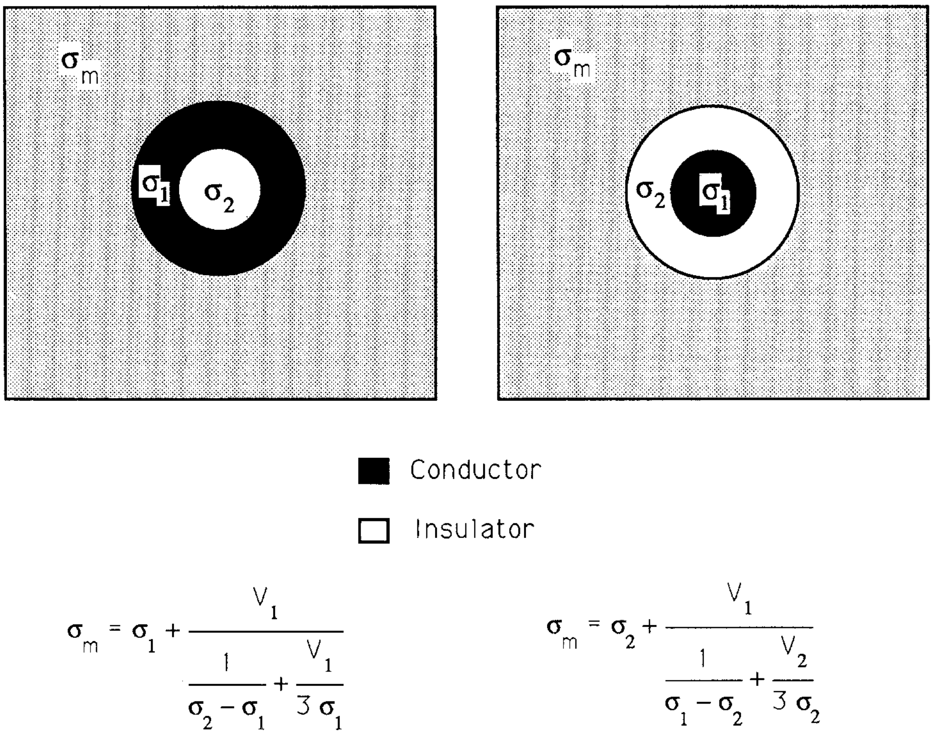

$$\sigma_m = \sigma_1 + \frac{V_1}{\dfrac{1}{\sigma_2 - \sigma_1} + \dfrac{V_1}{3\sigma_1}} \qquad \sigma_m = \sigma_2 + \frac{V_1}{\dfrac{1}{\sigma_1 - \sigma_2} + \dfrac{V_2}{3\sigma_2}}$$

Figure 5 Geometrical representation of composite phases used for the construction of Hashin–Shtrickman's bounds.

TABLE I Experimental and theoretical (Landauer's model [9]) electrical resistivity values of the different composites elaborated.

	ZrO$_2$3Y12	TiC$_{1-x}$N$_x$		Sintering temperature (°C)	Vol % m-ZrO$_2$ after sintering	Experimental electrical resistivity (μΩ cm)	Resistivity calculated with Landauer's model [9] (μΩ cm)
	Vol %		x				
1	13	87	0	1690	0	93 ± 1	87
2	4	96	1	1640	0	45 ± 1	43
3	56	44	0	1390	4	830 ± 78	438
4	50	50	1	1400	0	280 ± 18	160
5	10	90	0.5	1650	0	75 ± 1	60
6	34	66	0	1500	10	325 ± 30	143
7	26.5	73.5	1	1460	0	105 ± 2	66
8	54	46	0.5	1450	2	475 ± 10	268
9	33	67	0.5	1550	0	187 ± 5	100
10	21	79	0.33	1550	0	88 ± 2	82
11	43	57	0.33	1480	0	235 ± 9	158
12	18.5	81.5	0.67	1600	0	90 ± 2	64
13	42	58	0.67	1500	0	183 ± 5	126

TABLE II Fractional factorial matrix 2^{4-1} used to determine the effect of the hot-pressing parameters on the electrical resistivity of a TiC$_{0.33}$N$_{0.67}$–50% Z3Y6 composite

	Cooling rate (°C min^{-1})	Sintering temperature (°C)	Soaking time (min)	Pressure (MPa)	m-ZrO$_2$ content (vol %) after sintering	Electrical resistivity (μΩ cm)
1	10	1500	20	20	2	670 ± 84
2	30	1500	20	40	6	935 ± 90
3	10	1700	20	40	0	240 ± 10
4	30	1700	20	20	0	690 ± 55
5	10	1500	60	40	12	880 ± 120
6	30	1500	60	20	0	840 ± 60
7	10	1700	60	20	0	250 ± 8
8	30	1700	60	40	0	290 ± 18

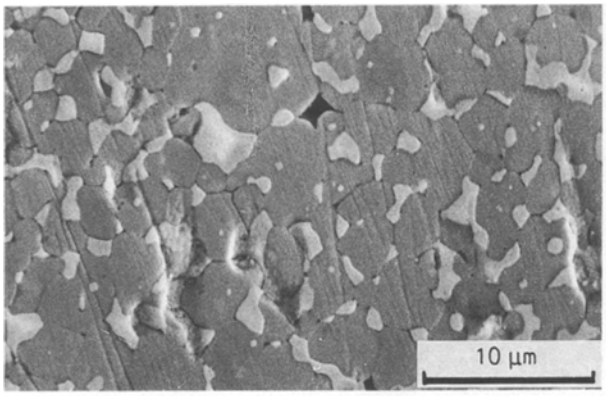

Figure 7 Microstructure of a TiC$_{0.67}$N$_{0.33}$–21 vol % ZrO$_2$ composite sintered at 1700 °C.

Figure 8 Fracture facies of a TiC$_{0.67}$N$_{0.33}$–21 vol % ZrO$_2$ composite sintered at 1550 °C.

Finally, in the case of this study, the conductivity σ_m of the TiC$_{1-x}$N$_x$–ZrO$_2$ composites should be described by the following equation:

$$\sigma_m = [(1 - x)\sigma_{TiC} + x\sigma_{TiN}]\left[\frac{3V_{TiCN} - 1}{2}\right] \quad (4)$$

Table I shows relatively important discrepancies between the experimental results and those obtained with the phenomenological equation. These discrepancies are larger when monoclinic zirconia is detected after sintering (Nos 3 and 6) and when zirconia content increases or sintering temperature decreases. The microcracks due to the tetragonal–monoclinic zirconia transformation hinder the electric current passage.

Table II shows that the resistivity of a TiC$_{0.33}$N$_{0.67}$–50 % ZrO$_2$ composite can vary with the hot-pressing parameters. Sintering temperature has the most important influence on the resistivity of the material, and this property can decrease from an average value of 220 μΩ cm with an increase of 100 °C in sintering temperature. The theoretical resistivity obtained with the Landauer model (240 μΩ cm) is reached only with the highest temperature.

At low sintering temperature, the cohesion between

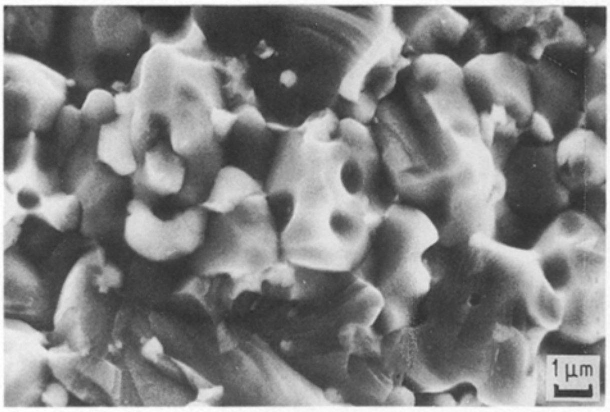

Figure 9 Facture facies of a $TiC_{0.67}N_{0.33}$–21 vol % ZrO_2 composite sintered at 1700 °C.

the non-oxide grains is weak and forms a barrier against the current passage, and the conductivity of the material decreases. Furthermore a residual porosity of 2% is always detected, and is situated at the grain boundaries between titanium carbonitride particles which constitute traps for the electrons (Fig. 7). Fracture facies of $TiC_{0.67}N_{0.33}$–21% ZrO_2 samples hot-pressed at 1550 and 1700 °C have been compared (Figs 8 and 9). The sample sintered at 1550 °C has an intergranular fracture that points out a non-cohesive interface (Fig. 8). The fracture facies of TiCN grains at 1700 °C are essentially intragranular, hence the interface between TiCN grains is strong (Fig. 9) and electric current passage is easier at this temperature. The same fracture facies give evidence of a grain growth when the temperature increases from 1550 to 1700 °C. Hence the grain boundary density in a volume unit is lower when the temperature increases. Grain boundaries often hinder the electric current passage, which also explains why the conductivity increases with sintering temperature. Furthermore, a high nitrogen content and a high sintering temperature stabilize tetragonal zirconia, thus no microcracking occurs [6].

To verify the validity of Landauer's equation, samples are now elaborated at 1700 °C to obtain a cohesive interface between TiCN grains. To avoid the zirconia transformation, it is necessary to add 5 mol % of yttria.

Free from the phenomena modifying resistivity, the latter follows the Landauer model with a good approximation (Table III). In Fig. 10, isoresistivity curves generated with this model are plotted. The composites containing the highest zirconia content deviated most from the model because here a little error on the volumic fraction can lead to an important difference in the resistivity value.

In another example (SiC–ZrB_2 ceramic composites), the authors have studied the influence of the dispersion of ZrB_2 particles in a modified Landauer's model [10, 11].

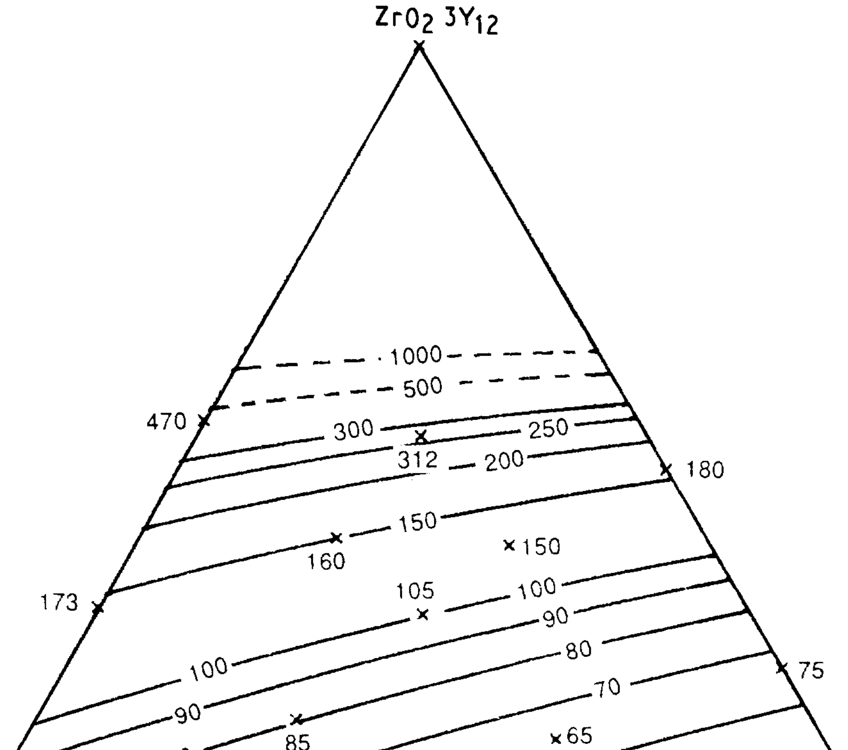

Figure 10 Electrical isoresistivity curves (μΩ cm) plotted with Landauer's equation and experimental results for 13 compositions hot-pressed at 1700 °C.

TABLE III Experimental and theoretical (Landauer's model [9]) electrical resistivity values of the different composites elaborated at 1700 °C under 40 MPa for 30 min.

	ZrO_25Y12	$TiC_{1-x}N_x$		Experimental electrical resistivity (μΩ cm)	Resistivity calculated with Landauer's model [9] (μΩ cm)
	Vol %		x		
1	13	87	0	93 ± 1	87
2	4	96	1	45 ± 1	43
3	56	44	0	470 ± 5	438
4	50	50	1	180 ± 3	160
5	10	90	0.5	73 ± 1	60
6	34	66	0	173 ± 2	143
7	26.5	73.5	1	75 ± 2	66
8	54	46	0.5	312 ± 5	268
9	33	67	0.5	105 ± 1	100
10	21	79	0.33	85 ± 2	82
11	43	57	0.33	160 ± 3	158
12	18.5	81.5	0.67	65 ± 1	64
13	42	58	0.67	150 ± 2	126

5. Conclusions

The electrical conductivity of the $TiC_{1-x}N_x$–ZrO_2 composite was studied. This property can be described using Landauer's model, because the microstructure of the composite is similar to those utilized to build this model. Strong deviations from the theoretical values were observed for experimental results under some conditions. At low sintering temperatures, the residual porosity and non-cohesive interfaces between the grains of the conductive phase hinder the passage of the electric current. Microcracks resulting from zirconia transformation also constitute a barrier against the electron passage.

Acknowledgements

This work is part of the PhD of E. Barbier, Ecole des Mines de Saint-Etienne, France, no. S3TD, 1991.

References

1. L. E. TOTH, "Transition Metal Carbides and Nitrides, Refractory Materials", (Academic, New York, 1971).
2. T. WATANABE, T. DOUTSU, K. SHOUBU and Y. KAI *Mater. Sci. Forum* **34–36** (1988) 561.
3. H. PASTOR, *Mater. Sci. Engng* **A105/106** (1988) 401.
4. T. WATANABE, H. YAMAMOTO, K. SHOBU, T. SAKAMOTO, *J. Amer. Ceram. Soc.* **71** (1988) C202.
5. E. BARBIER and F. THEVENOT *Silicates Industriels* **7–8** (1990) 181.
6. *Idem, J. Eur. Ceram. Soc.* **8** (1991).
7. O. WIENER, *Abh. Sachs. Ges. (akad.) Wiss.* **32** (1912) 509.
8. Z. HASHIN and S. SHTRIKMAN, *J. Appl. Phys.* **33** (1962) 3125.
9. R. LANDAUER, *J. Appl. Phys.* **23** (1952) 779.
10. R. JIMBOU, K. TAKAHASHI, Y. MATSUSHITA and T. KOSUGI, *Adv. Ceram. Mater.* **1** (1986) 341.
11. K. TAKAHASHI and R. JIMBOU, *J. Amer. Ceram. Soc.* **70** (1987) C369.

Received 7 January
and accepted 7 June 1991